Radio Science, Volume 16, Number 6, pages 1385–1400, November–December 1981

An analysis of short pulse and dual frequency radar techniques for measuring ocean wave spectra from satellites

Frederick C. Jackson

NASA Goddard Space Flight Center, Greenbelt, Maryland 20771

(Received September 16, 1980; revised June 8, 1981; accepted June 8, 1981.)

A four-frequency moment characterization of backscatter from the near-vertical is applied to an analysis of the short pulse (SP) and dual frequency (DF) microwave techniques. It is found that (1) the range reflectivity modulation spectrum closely approximates the directional wave slope spectrum. Harmonic distortion is small and is a minimum near 10° incidence. (2) The SP measurement SNR (signal-to-noise ratio) is typically 20–30 dB greater than the narrowband DF SNR. The difference in SNR is the ratio of the range beam extent to pulse length, minus the ratio of beam-limited to pulse-limited Doppler spreads. It is concluded that narrowband DF measurements are basically impractical. To be practical, the DF technique must be 'widebanded.' SP measurements on the other hand are found to be practical, using existing space-qualified microwave hardware.

INTRODUCTION

In this paper we consider the possibility of measuring the directional height spectrum of ocean wind-waves using relatively simple, scanning-beam microwave radars. With reference to Figure 1, consider a radar translating with velocity V over a statistically homogeneous sea, its beam pointing downward at some angle θ from the vertical and executing a slow conical scan. If the antenna beam spot on the surface is broad compared with the scale of the waves, then, obviously, unless one resorts to synthetic aperture, the waves cannot be resolved in azimuth. Rather, the reflectivity variations associated with the large wave structure will be averaged laterally across the beam. Now imagine a Fourier decomposition of the reflectivity pattern into component plane waves; recognize that the effect of the lateral averaging will be to eliminate or 'cancel out' any plane surface contrast wave that is not aligned with the beam direction. In other words, only that surface wave whose phase front is 'matched' to the electromagnetic phase front can survive the lateral averaging. Thus an harmonic component of the range reflectivity modulation detected by the radar must be due to a plane surface contrast wave having a wave vector $\mathbf{K}$ that is parallel to the radar line of sight. Further, the frequency of the modulation ω and the surface wave number $K = |\mathbf{K}|$ must be related by the two-way time delay:

$$K = (2\omega/c) \sin\theta \tag{1}$$

Now, what is the mechanism of reflectivity variation, and how do we propose to detect the range reflectivity modulation or measure its spectrum? The reflectivity modulation mechanism depends on incidence angle. Near vertical incidence $\theta \lesssim 15°$, microwave backscatter from the sea occurs by means of quasi-specular retroreflections from wave facets oriented normal to the radar line of sight. At large angles $\theta \gtrsim 25°$, the backscatter is due to a Bragg-type of resonant diffraction from short gravity or gravity-capillary waves whose wave vectors satisfy the identical relationship (1) if ω is understood to be the carrier frequency rather than the modulation frequency. In the transition region $\theta \sim 15°$–$25°$, both specular reflection and diffraction are important in the backscatter process. For a recent review of the theory of radar sea-return see *Valenzuela* [1978].

Now it is important to realize that the phase-front matching results in very high directional resolution ($\sim 1°$ in azimuth typically as we shall see). Hence, the range reflectivity modulation spectrum $P_{\text{mod}}(K, \Phi)$ in any given azimuth direction represents only a very narrow slice through the two-dimensional surface wave number spectrum, and a complete picture of the surface spectrum can therefore only be obtained by scanning the radar in azimuth. At satellite altitudes this scan can easily occupy many

Paper number 1S0983.

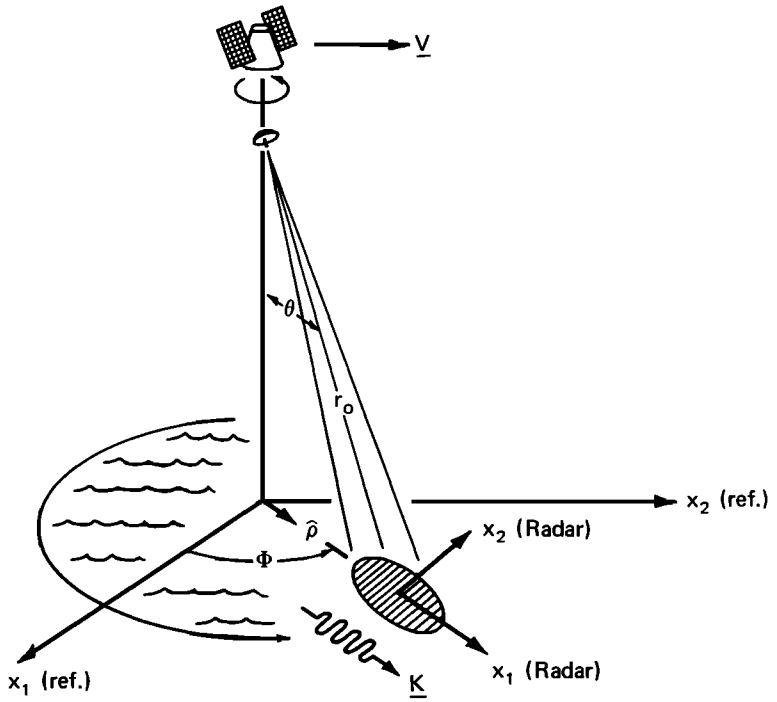

Fig. 1. Overall geometry and coordinate definition.

hundreds of kilometers if the nadir angle θ is not small. If the wavefield is not homogeneous over this distance, it will be impossible to assemble from the various azimuth looks a meaningful directional spectrum representative of a given ocean area. To be reasonably assured of homogeneous conditions the nadir angle must be small. For example, if θ = 10° and the altitude is 600 km then the radius of the scan is ~100 km. Since the wave number spectrum is polar-symmetric, it can be mapped in a ~1° square by scanning (at a 4 rpm rate, or greater) 180° on either side of the subsatellite track. A 1° square is a reasonably small area for the open ocean and happens to be the basic grid spacing of operational wave forecast models.

Thus our concern in this work is with small angles of incidence, and here we find ourselves fortunate for the reflectivity modulation mechansim in small-angle, specular backscatter is basically a purely geometrical tilting effect and is therefore amenable to accurate modeling without resort to empirical hydrodynamic modulation transfer functions. This is because the population of specularly reflecting facets derives from the entire wave ensemble, including waves on all scales, from the scale of the dominant waves we seek to measure down to the scale of the diffraction limit. For this large ensemble of waves it is reasonable to suppose that hydrodynamic forcing and wave-wave interaction effects are negligible, at least in the first order of approximation, and that therefore the surface should be describable as a free-wave superposition possessing Gaussian statistics. This situation is to be contrasted with large-angle backscatter, where strong and essentially unpredictable hydrodynamic modulation of the centimetric Bragg water wave is chiefly responsible for the electromagnetic modulation [*Wright et al.*, 1980]. The geometrical tilt mechanism in near-vertical backscatter is illustrated in Figure 2. According to this model, the reflectivity modulation is proportional to the large-wave slope component in the plane of incidence. It follows then that the range reflectivity modulation spectrum $P_{\text{mod}}(K, \Phi)$ is directly proportional to the large-wave directional slope spectrum $K^2F(K, \Phi)$, where F is the directional height spectrum. In this work we will show that the simple tilt model of Figure 2 provides a basically correct description of the modulation mechanism. It will be shown that the tilt model corresponds to the first and dominant term

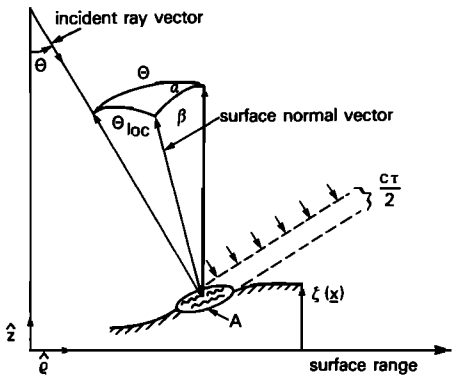

The fractional backscatter cross-section variation is

$$\frac{\delta\sigma}{\sigma} = \frac{\delta(\sigma^o A)}{\sigma^o A} = \frac{\delta\sigma^o}{\sigma^o} + \frac{\delta A}{A}$$

Assume that $\sigma^o = \pi \sec^4\Theta\, p(s)$ where $s = \tan\Theta_{loc}$ and p is the slope pdf. From the spherical triangle, if $\Theta >> \beta$, it follows that $\Theta_{loc} \sim \Theta - \beta\cos\alpha$, or $\Theta_{loc} \sim \Theta - \hat{\beta}\cdot\nabla\zeta$. Since $A \propto c\tau/2\sin\Theta_{loc}$ it follows that

$$\frac{\delta\sigma}{\sigma} = \left(\cot\Theta - \frac{\partial \ell n p}{\partial s}\right)\hat{\rho}\cdot\nabla\zeta$$

Fig. 2. Simple tilt model of reflectivity modulation.

in a geometrical optics series expansion of P_{mod} in which the large-wave steepness is the fundamental ordering parameter.

In principle, the range modulation spectrum can be measured by either short pulse (SP) or dual frequency (DF) techniques. In the SP technique, very short pulses are used to resolve the wave structure in range. Most simply, $P_{mod}(\omega, \Phi)$ is obtained by spectrum-analyzing the video output of an envelope detector. In the DF technique first proposed by *Ruck et al.* [1972], quasi-monochromatic waveforms that entirely fill the beam spot on the surface are transmitted at two closely separated microwave frequencies. An harmonic surface contrast modulation is detected through the interaction of the 'beat wave' with the surface. Most simply, $P_{mod}(\omega, \Phi)$ is obtained by cross correlating the powers backscattered in the two frequencies ν and $\nu - \omega$. *Jackson* [1974] pointed out that on account of the narrowband nature of the transmitted waveforms, the DF signal, the covariance of powers, will be small compared with the variance of power in either frequency. This is because the sea-slope spectrum is basically broadband, having a bandwidth of 50–100% of the peak frequency, whereas the analysis bandwidth δK in the DF measurement is comparatively narrowband, being equal to the reciprocal of the range beam extent—the 'record length.' Hence the correlation coefficient, or the SNR $\equiv P_{mod}(K)\delta K$, will be quite small when the footprint dimensions are large. Borrowing from the detection theory work of *Parzen and Shiren* [1956], *Jackson* [1974] showed how the SNR (signal-to-noise ratio) in the DF measurement technique could be greatly enhanced by using wideband signals (e.g., by using short pulses). By widening the analysis bandwidth, Jackson showed that the DF SNR could be raised to levels comparable to typical SP SNRs.

Alpers and Hasselmann [1978] (hereinafter referred to as A-H), rather than using wideband signals to improve the DF SNR as suggested by *Jackson* [1974] instead introduced the idea of slow-time filtering the complex DF signal,

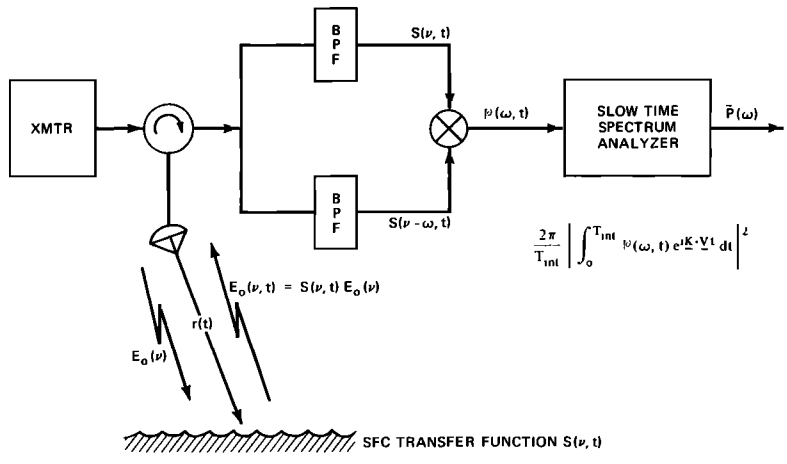

Fig. 3. Schematic of a dual frequency system.

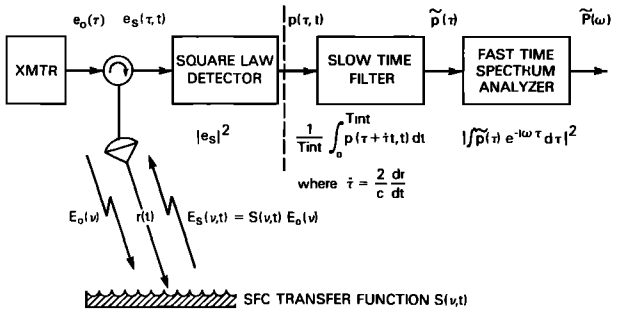

Fig. 4. Possible realization of a short pulse system. τ denotes fast signal time and t slow signal time. The slow time filter can be realized by a sample-and-hold that is triggered at successive delays given by $\dot{\tau}t$, followed by an accumulator. The spectrum analyzer can be realized by digitally fast Fourier transforming the slow time filtered pulse return, and squaring the magnitude.

$$\mathscr{P}(\omega, t) = S(\nu, t)S^*(\nu - \omega, t) \tag{2}$$

where the S are the signals backscattered at the two frequencies. A-H showed that if $\mathscr{P}(\omega, t)$ is filtered at the Doppler shift frequency of the modulation $\Omega = \mathbf{K} \cdot \mathbf{V}$, then (according to their large-angle analysis) satellite measurement SNRs typically of $\sim$+3 dB could be obtained. Hence satellite measurement feasibility was indicated. A DF system employing the A-H filtering concept is schematically illustrated in Figure 3.

In this work we show that the A-H filtering is functionally identical to pulse integration in a SP system. Thus, to drive down the level of random signal fading caused by the waveform coherency, backscattered pulses are integrated in surface-fixed range bins prior to spectrum analysis for the range modulation. An illustration of such a SP system is given in Figure 4. Following, the DF and SP systems of Figures 3 and 4 are analyzed in the frequency domain. (Space does not permit a like analysis of various possible wideband DF systems.) The ensemble average outputs of the two systems are expressed in terms of the common 'four-frequency' moment of the surface scattering transfer function. A solution for the moment is obtained by using physical optics in the high-frequency, geometrical optics scattering limit, and this solution is applied to an SNR analysis of the two systems.

SYSTEMS ANALYSIS

As the narrowband DF analysis results follow immediately from the moment results in the wideband analysis problem, let us first consider the SP system of Figure 4. Let τ denote fast signal time (time scale of microseconds), and let t denote slow signal time (time scale of milliseconds). Let $e_0(\tau)$ represent the incident field waveform arriving at the beam spot center, and let the Fourier transform (FT) of e_0 be

$$E_0(\nu) = \frac{1}{2\pi}\int e^{-i\nu\tau} e_0(\tau)\,d\tau \tag{3}$$

The backscattered field $e_s(\tau, t)$ is a duration-limited random process in fast time τ (the duration being determined by the round-trip travel time of an impulse across the beam spot on the surface) and is assumed to be a stationary random process in slow time t. Stationarity in t follows if the beam is translating at a uniform velocity across the surface. Thus it is implicitly assumed that the azimuth Φ is fixed during the measurement integration time. Further, it is assumed that the pulse repetition frequency (PRF) is greater than the Doppler fading rate so that $e_s(\tau, t)$ can be treated as a continuous function of t. If the FT of $e_s(\tau, t)$ with respect to τ is $E_s(\nu, t)$ then

$$E_s(\nu, t) = S(\nu, t)E_0(\nu) \tag{4}$$

where $S(\nu, t)$ is the surface scattering transfer function. The output of the square-law detector is $p(\tau, t) = |e_s(\tau, t)|^2$. If $\mathscr{P}(\omega, t)$ is the FT of p with respect to τ, then

$$\mathscr{P}(\omega, t) = \int_{-\infty}^{\infty} E_s(\nu, t)E_s^*(\nu - \omega, t)\,d\nu \tag{5}$$

where the asterisk denotes the complex conjugate. The pulse spectrum is defined as $P(\omega) = \langle|\mathscr{P}(\omega, t)|^2\rangle$ where the angle brackets denote ensemble average. The filter in Figure 4 functions to integrate pulse returns in surface-fixed range bins. The output of the filter after an integration time T_{int} is

$$\bar{p}(\tau) = \frac{1}{T_{int}}\int_0^{T_{int}} p(\tau + \dot{\tau}t, t)\,dt \tag{6}$$

where the rate of change of signal delay $\dot{\tau} = (2/c)\,dr/dt$, r being the range to the surface. The spectrum of the filtered pulse return $\bar{p}(\omega)$ is defined as $\bar{P}(\omega) = \langle|\bar{\mathscr{P}}(\omega)|^2\rangle$ where $\bar{\mathscr{P}}(\omega)$ is the FT of $\bar{p}(\tau)$. The spectrum $\bar{P}(\omega)$ can be expressed as

$$\bar{P}(\omega) = \int_{-\infty}^{\infty} W(\Omega - \mathbf{K}\cdot\mathbf{V})P(\omega, \Omega)\,d\Omega \tag{7}$$

where the Doppler frequency $\Omega = \mathbf{K} \cdot \mathbf{V} = \omega\dot{\tau}$

and where the filter window

$$W(\Omega) = \left[\frac{\sin(\Omega T_{int}/2)}{(\Omega T_{int}/2)}\right]^2 \tag{8}$$

and $P(\omega, \Omega)$ is the post-detection pulse-Doppler spectrum defined by

$$P(\omega, \Omega) = \frac{1}{2\pi}\int_{-\infty}^{\infty} \langle \mathscr{P}(\omega, t)\mathscr{P}^*(\omega, t + \Delta t)\rangle e^{i\Omega\Delta t} d\Delta t \tag{9}$$

If the generalized, 'four-frequency' moment is defined as

$$M(\nu, \nu', \omega; \Delta t) = \langle S(\omega, t)S^*(\nu - \omega, t) \cdot S^*(\nu', t + \Delta t)S(\nu' - \omega, t + \Delta t)\rangle \tag{10}$$

and the FT of M with respect to Δt,

$$N(\nu, \nu', \omega; \Omega) = \frac{1}{2\pi}\int_{-\infty}^{\infty} M(\nu, \nu', \omega; \Delta t) e^{i\Omega\Delta t} d\Delta t \tag{11}$$

then

$$P(\omega, \Omega) = \int\int_{-\infty}^{\infty} N(\nu, \nu', \omega; \Omega) E_0(\nu) \cdot E_0^*(\nu - \omega)E_0^*(\nu')E_0(\nu' - \omega) d\nu\, d\nu' \tag{12}$$

Now consider the DF system of Figure 3. If the incident fields $E_0(\nu)$ and $E_0(\nu - \omega)$ are assumed to have unit amplitudes, then the complex signal out of the mixer $\mathscr{P}(\omega, t)$ is given by (2). From the definitions (9)–(11) the spectrum of the DF signal $\mathscr{P}(\omega, t)$ is evidently given by N with $\nu = \nu'$. If a finite record of length T_{int} is passed to the spectrum analyzer, then the ensemble average output will be

$$\bar{P}(\omega) = \int_{-\infty}^{\infty} W(\Omega - \mathbf{K}\cdot\mathbf{V}) N(\nu, \nu, \omega; \Omega) d\Omega \tag{13}$$

MOMENT SOLUTION (FAR ZONE)

Here it is convenient to deal in terms of wave number $k = \nu/c$, etc. For now and for future reference let us establish the identities

$$\nu = kc,\ \nu' = k'c,\ \omega = \kappa c$$
$$\Delta\nu = \nu - \nu',\ \Delta k = \Delta\nu/c = k - k' \tag{14}$$

We will move freely in the remainder of this paper between wave number and frequency domain representations and will not bother to modify functional forms (e.g., $S(k)$ is taken to be the same as $S(\nu)$). The physical optics integral solution for the transfer function is (e.g., assuming perfect conductivity [cf. *Beckmann and Spizzichino*, 1963]):

$$S(k, t) = \frac{ik\sec\theta}{2\pi r_0}\int G(\mathbf{x} - \mathbf{V}t)\exp[-i2kr(\mathbf{x}, t)]\, d\mathbf{x} \tag{15}$$

where G is the illumination pattern, $\mathbf{x} = (x_1, x_2)$ is the coordinate vector of surface points in a surface-fixed reference frame, $d\mathbf{x} = dx_1 dx_2$ is the element of horizontal area, and where the integration extends over the illuminated area. The origin of the coordinate system $\mathbf{x} = \mathbf{0}$ is taken to coincide with the center of the beam spot at $t = 0$. For small t, the Fresnel approximation to the phase is valid,

$$-2kr(\mathbf{x}, t) \simeq -2kr_0 + 2k\cos\theta\zeta(\mathbf{x}) - 2k\sin\theta\hat{\boldsymbol{\rho}} \cdot (\mathbf{x} - \mathbf{V}t) + (k/r_0)\{|\mathbf{x} - \mathbf{V}t|^2 - \sin^2\theta \cdot [\hat{\boldsymbol{\rho}}\cdot(\mathbf{x} - \mathbf{V}t)]^2 + \zeta^2(\mathbf{x})\} \tag{16}$$

where $\zeta(\mathbf{x})$ is the random wave height and $\hat{\boldsymbol{\rho}}$ is the unit vector in the horizontal pointing in the direction of increasing range.

Before we attempt a calculation of the time-lagged moment (10) in the Fresnel approximation, let us first consider the simpler problem of calculating the moment for zero time lag only in the far-zone approximation to the phase. By starting with the simpler problem, we will be able to comprehend the basic scattering physics more clearly; also, once having the far-zone solution in hand we will be better able to deal with the complications introduced by the Fresnel phase factors. Retaining only the first three plane wave terms in (16) we get on forming the moment $M \equiv M(k, k', \kappa; 0)$ assuming the interchangeability of expectation and integration operations, and ignoring the time dependence which is trivial without the Fresnel terms:

$$M(k, \Delta k, \kappa) = \left(\frac{k\sec\theta}{2\pi r_0}\right)^4 \int_{-\infty}^{\infty}\cdots\int G(\mathbf{x}^1)\cdots G(\mathbf{x}^4) \cdot \langle \exp\{i2\cos\theta[k(\zeta^1 - \zeta^2 - \zeta^3 + \zeta^4) + \Delta k(\zeta^3 - \zeta^4) + \kappa(\zeta^2 - \zeta^4)]\}\rangle \cdot \exp\{-i2\sin\theta\hat{\boldsymbol{\rho}} \cdot [k(\mathbf{x}^1 - \mathbf{x}^2 - \mathbf{x}^3 + \mathbf{x}^4) + \Delta k(\mathbf{x}^3 - \mathbf{x}^4) + \kappa(\mathbf{x}^2 - \mathbf{x}^4)]\}\, d\mathbf{x}^1\cdots d\mathbf{x}^4 \tag{17}$$

where $\zeta^1 = \zeta(\mathbf{x}^1)$ etc. The geometrical optics $k \to \infty$ limit of (17) is taken according to a method described by *Barrick* [1968] in connection with the limit of the second moment $\langle |S(k)|^2 \rangle$ (i.e., the average backscattered power). For large k (i.e., for large rms phase variation $2k \cos \theta \langle \zeta^2 \rangle^{1/2}$), it is apparent that appreciable contributions to the moment are made only in the neighborhoods of two sets of stationary points, viz.,

$$\mathscr{S}_1 : \mathbf{x}^1 = \mathbf{x}^2, \mathbf{x}^3 = \mathbf{x}^4$$
$$\mathscr{S}_2 : \mathbf{x}^1 = \mathbf{x}^3, \mathbf{x}^2 = \mathbf{x}^4 \tag{18}$$

Except where $\mathbf{x}^1 = \mathbf{x}^2 = \mathbf{x}^3 = \mathbf{x}^4$, the sets $\mathscr{S}_1$ and $\mathscr{S}_2$ are distinct and yield distinct contributions to the moment; i.e., $M = M_1 + M_2$ where M_1 and M_2, respectively, derive from integrations over the small volumes surrounding $\mathscr{S}_1$ and $\mathscr{S}_2$. Consider the integration over the volume containing $\mathscr{S}_1$. Let

$$\mathbf{u} = 2k \cos \theta(\mathbf{x}^1 - \mathbf{x}^2)$$
$$\mathbf{v} = 2k \cos \theta(\mathbf{x}^3 - \mathbf{x}^4)$$
$$\mathbf{w} = \mathbf{x}^2 - \mathbf{x}^4$$
$$\mathbf{x} = \mathbf{x}^4 \tag{19}$$

Now expand the height differences in the neighborhoods of the stationary points $\mathscr{S}_1$ in a Taylor series,

$$2k \cos \theta(\zeta^1 - \zeta^2) = \nabla\zeta^2 \cdot \mathbf{u} + 0(u^2/k)$$
$$2k \cos \theta(\zeta^3 - \zeta^4) = \nabla\zeta^4 \cdot \mathbf{v} + 0(v^2/k) \tag{20}$$

where $\nabla \equiv (\partial/x_1, \partial/\partial x_2)$. Then the contribution M_1 to M for large k becomes

$$M_1 \sim (2r_0 \cos^2 \theta)^{-4} \int A(\mathbf{w}) \exp(-i2k \sin \theta \hat{\boldsymbol{\rho}} \cdot \mathbf{w}) d\mathbf{w}$$
$$\times \{(2\pi)^{-4} \int\int \langle \exp\{i[\nabla\zeta^2 \cdot \mathbf{u} - \nabla\zeta^4 \cdot \mathbf{v}$$
$$+ 2\kappa \cos \theta(\zeta^2 - \zeta^4) + 0((u^2 + v^2)/k) + 0(\Delta k v/k)]\}\rangle$$
$$\cdot \exp\{i[\tan \theta \hat{\boldsymbol{\rho}} \cdot (\mathbf{u} - \mathbf{v}) + 0(\Delta k v/k)]\} d\mathbf{u} d\mathbf{v}\} \tag{21}$$

where in (21) we have already taken the large k limit in the products of the gains, i.e., we have let $G(\mathbf{x}^1) \cdots G(\mathbf{x}^4) \sim G^2(\mathbf{x} + \mathbf{w})$ and where we have integrated over the remaining space variable $\mathbf{x}$, letting $A(\mathbf{w})$ represent the convolved two-way gain pattern:

$$A(\mathbf{w}) = \int_{-\infty}^{\infty} G^2(\mathbf{x}) G^2(\mathbf{x} + \mathbf{w}) d\mathbf{x} \tag{22}$$

Now consider the limit of the factor in braces as $k \to \infty$. Let $\boldsymbol{\xi}$ denote the random six-vector,

$$\boldsymbol{\xi} = (\nabla\zeta^2, \nabla\zeta^4, \zeta^2, \zeta^4) \tag{23a}$$

and let $\mathbf{t}$ denote the associated six-dimensional characteristic vector,

$$\mathbf{t} = (\mathbf{u}, -\mathbf{v}, 2\kappa \cos \theta, -2\kappa \cos \theta) \tag{23b}$$

The characteristic function of $\boldsymbol{\xi}$ is defined as

$$\psi_{\xi}(\mathbf{t}; \mathbf{w}) = \langle e^{i\mathbf{t}\cdot\boldsymbol{\xi}} \rangle = \int e^{i\mathbf{t}\cdot\boldsymbol{\xi}} p_{\xi}(\boldsymbol{\xi}; \mathbf{w}) d\boldsymbol{\xi} \tag{24}$$

where p_{ξ} is the pdf (probability density function) of $\boldsymbol{\xi}$. Since $\zeta(\mathbf{x})$ is a stationary process, the pdf and characteristic function depend only on the separation, or lag vector $\mathbf{w} = \mathbf{x}^2 - \mathbf{x}^4$. From these definitions we have for M_1 in the high-frequency limit,

$$\lim_{k\to\infty} M_1 \equiv M_1(\kappa) = (2r_0 \cos \theta)^{-4}$$
$$\cdot \int A(\mathbf{w}) \exp(-i2\kappa \sin \theta \hat{\boldsymbol{\rho}} \cdot \mathbf{w}) d\mathbf{w}$$
$$\times \{(2\pi)^{-4} \int\int \psi_{\xi}(\mathbf{t}; \mathbf{w}) \exp[-i \tan \theta \hat{\boldsymbol{\rho}}$$
$$\cdot (\mathbf{u} - \mathbf{v})] d\mathbf{u} d\mathbf{v}\} \tag{25}$$

Since M_1 in the large k limit is a function of κ only and the total moment $M = M_1 + M_2$, and since M is symmetric with respect to a κ and Δk interchange, then we must have

$$\lim_{k\to\infty} M(k, \Delta k, \kappa; 0) = M_1(\kappa) + M_1(\Delta k) \tag{26}$$

Note that the limit does not have to be taken in order that (26) hold true approximately.

Now let us define the surface wave vector $\mathbf{K}$ and specular slope vector $\mathbf{s}$,

$$\mathbf{K} = 2\kappa \sin \theta \hat{\boldsymbol{\rho}}$$
$$\mathbf{s} = \tan \theta \hat{\boldsymbol{\rho}} \tag{27}$$

and let us write the solution (26) as

$$M_1(\mathbf{K}) = (2r_0 \cos^2 \theta)^{-4}$$
$$\cdot \int_{-\infty}^{\infty} A(\mathbf{w}) \Xi(K; \mathbf{w}) \exp(-i\mathbf{K} \cdot \mathbf{w}) d\mathbf{w} \tag{28}$$

where Ξ represents the factor in braces, viz.,

$$\Xi(K; \mathbf{w}) = (2\pi)^{-4} \int\int_{-\infty}^{\infty} \psi_{\xi}(\mathbf{u}, -\mathbf{v}, K \cot \theta,$$
$$-K \cot \theta; \mathbf{w}) \exp[-i\mathbf{s} \cdot (\mathbf{u} - \mathbf{v})] d\mathbf{u} d\mathbf{v} \tag{29}$$

An alternative form of the solution may be obtained by using (24) for ψ_{ξ} and integrating over $\mathbf{u}$ and $\mathbf{v}$:

$$\Xi(K; \mathbf{w}) = \int\int_{-\infty}^{\infty} p_{\xi}(\mathbf{s}, \mathbf{s}, \zeta^2, \zeta^4; \mathbf{w}) \cdot \exp\,[iK \cot\theta(\zeta^2 - \zeta^4)]\, d\zeta^2 d\zeta^4 \tag{30}$$

For future reference let us write down here the result for the second moment. Using the same method we have used for the limit of the fourth moment, we have

$$\lim_{k\to\infty} \langle |S(k)|^2 \rangle = \left(\frac{A_0 \sec^4\theta}{4r_0^2}\right) p_{\nabla\zeta}(\mathbf{s}) \tag{31}$$

where $A_0 = \int G^2 d\mathbf{x}$. The limiting form (31) provides a good fit to near vertical backscatter data provided some account is made of diffraction for finite k. Diffraction can be accounted for by treating $p_{\nabla\zeta}$ as though it were the pdf of slopes in a smoothed sea surface in which waves smaller than the diffraction limit have been removed by a spatial filter [*Brown*, 1978]. If the limiting cross section form $\sigma^\circ = \pi \sec^4\theta\, p_{\nabla\zeta}(\mathbf{s})$ is fitted to the 2-cm cross-section data of *Jones et al.* [1977] one finds that $p_{\nabla\zeta}$ is approximately Gaussian with a slope variance $m_0^2 \equiv \langle |\nabla\zeta|^2 \rangle$ that is approximately a linear function of windspeed U,

$$m_0^2 \underset{\text{(Ku-band)}}{\cong} 0.0025\, U\,[\text{m s}^{-1}] + 0.01 \tag{32}$$

Equation (32) gives slope variances in the windspeed range 10–25 m s^{-1} that are ~60% of the optical values reported by *Cox and Munk* [1954] and which, interestingly, lie between their 'clean' and 'slick' surface observations.

EXPANSION OF $M_1(\mathbf{K})$

We seek an expansion of the moment solution (27)–(30), basically in powers of the large wave steepness δ_0, such that the first-order term gives us what we are after, namely, the directional slope spectrum, and the higher-order terms give us the departure from direct proportionality to the slope spectrum. We will discover a posteriori that such an expansion is valid (i.e., that it converges rapidly for a sizeable range of the parameter values θ, m_0, and δ_0). $M_1(\mathbf{K})$ is expanded by first expanding $\Xi(K; \mathbf{w})$ as given by (29) and then term-by-term Fourier transforming with respect to $\mathbf{w}$. Ξ is expanded according to *Longuet-Higgins'* [1963] method for generating the non-Gaussian pdfs of variables in a weakly nonlinear sea.

As is well known, sea surface height and slope distributions are nearly Gaussian; what departures there are from normality can be accurately modelled with Gram-Charlier series representations. *Longuet-Higgins'* [1963] theory provides a rational means for generating these series based on the cumulant-generating and characteristic functions. Further, *Longuet-Higgins* [1963] shows how the coefficients of these series may be derived from the nonlinear water wave equations. For simplicity, we consider here statistics only up to third order. Then the characteristic function of ξ (cf. (23)–(25)) assumes the simple form,

$$\psi_{\xi}(\mathbf{t}; \mathbf{w}) = \exp\left[-\frac{1}{2}\mu_{ij}(\mathbf{w}) t_i t_j\right] \times \left[1 + \frac{i^3}{3!}\lambda_{ijk}(\mathbf{w}) t_i t_j t_k\right] \tag{33}$$

where the covariances $\mu_{ij} = \langle \xi_i \xi_j \rangle$ and the third moments $\lambda_{ijk} = \langle \xi_1 \xi_j \xi_k \rangle$. It is assumed that mean water level is zero so that $\langle \xi \rangle = \mathbf{0}$. The characteristic vector $\mathbf{t} = (t_i) = (\mathbf{u}, -\mathbf{v}, K \cot\theta, -K \cot\theta)$ and the Einstein summation convention applies to repeated indices. We note the obvious, that if ξ is perfectly normally distributed then the third moments λ_{ijk} vanish, and ψ_{ξ} is given by the normal form exp (—). The elements of the covariance matrix μ can be expressed in terms of the wave height covariance function,

$$R(\mathbf{w}) = \langle \zeta^2 \zeta^4 \rangle = \langle \zeta(\mathbf{x} + \mathbf{w})\zeta(\mathbf{x}) \rangle \tag{34}$$

or various derivatives thereof, as can be verified, for example, using methods outlined in *Papoulis* [1965]:

$$\mu = \begin{bmatrix} m_{\alpha\beta} & -R_{,\alpha\beta} & 0 & -R_{,\alpha} \\ & m_{\alpha\beta} & R_{,\alpha} & 0 \\ & & \sigma^2 & R \\ \text{symmetric} & & & \sigma^2 \end{bmatrix} \tag{35}$$

where we have defined $\sigma^2 = R(\mathbf{0})$, $R_{,\alpha} = \partial R(\mathbf{w})/\partial w_\alpha$ etc. and $m_{\alpha\beta} = -R_{,\alpha\beta}(\mathbf{0})$, and where α and β range from 1 to 2. The mean square slope $m_0^2 = m_{\alpha\alpha} = m_{11} + m_{22}$.

Let the large wave steepness $\delta_0 = K_0\sigma$ where K_0 is the wave number of the dominant wave. Characteristically $\delta_0 = 0.05$ for fully aroused seas, $\delta_0 = 0.1$ for developing seas, and $\delta_0 < 0.05$ for decaying seas. If $U = 10$ m s^{-1} then by (32) $m_0 = 0.2$ and so typically $\delta_0/m_0 \sim 0.25$. Let $\mu = \mu^d + \mu^0$ where d and o stand for the diagonal and

off-diagonal blocks of (35). For lags w removed from the origin, e.g., on the order of a quarter of a wavelength $\mu^0 = 0(\delta_0^2)$ whereas $\mu^d = 0(m_0^2)$, and so we can expand the normal form in (33) for small μ^0:

$$\psi_\xi \sim \exp\left(-\frac{1}{2}\mu_{ij}{}^d t_i t_j\right) \times \left[1 - \frac{1}{2}\mu_{ij}{}^0 t_i t_j - \frac{i}{6}\lambda_{ijk} t_i t_j t_k + \frac{1}{8}\mu_{ij}{}^0 \mu_{kl}{}^0 t_i t_j t_k t_l + \cdots\right] \tag{36}$$

Now similarly to (35) we expect that the λ_{ijk} are derivable from a knowledge of the lagged product function $Q(\mathbf{r}, \mathbf{s}) = \langle \zeta(\mathbf{x} + \mathbf{r})\zeta(\mathbf{x} + \mathbf{s})\zeta(\mathbf{x})\rangle$, the FT of which with respect to r and s is known as the bispectrum [*Hasselmann et al.*, 1963]. In principle, one may derive the bispectrum and hence the λ_{ijk} from the height spectrum, the FT of $R(\mathbf{w})$, using a Stokes' perturbation expansion of the nonlinear water wave equations according to the theories of *Longuet-Higgins* [1963] and *Hasselmann et al.* [1963]. The successful application of these theories to the prediction of the average impulse response at vertical incidence to 3 cm radiation by *Jackson* [1979] leads us to suppose that these theories may be useful in the present context. However, for obvious reasons, we will not attempt to model the λ satistics here. We merely point out their existence and call attention to their importance. For example, consider small values of $\tan\theta/m_0$. Then the height terms tend to dominate and the second-order μ^0 term is then $0(K^4 \cot^4\theta\sigma^4) = 0(\delta_0{}^4 \cot^4\theta)$. The corresponding λ term is $0(K^3 \cot^3\theta\lambda_0\sigma^3)$ where $\lambda_0 = \langle\zeta^3\rangle\sigma^{-3}$ is the height skewness coefficient. In general λ_0 and δ_0 are proportional to each other. From Longuet-Higgins' theory, if one assumes a Phillips spectral form, then $\lambda_0 = 4\delta_0$. This follows from *Jackson* [1979] if an error of a factor of 2 in the second-order height profile is corrected for, i.e., if $\zeta_2 \leftarrow \zeta_2/2$. Thus the λ term is $0(4\delta_0{}^4 \cot^3\theta)$ and is comparable to the second-order term in μ^0. Hence, a priori the neglect of the skewness statistics is unjustified. Nevertheless, to get on with the analysis we will assume a Gaussian surface model.

Writing out the characteristic function using (35) for the elements of μ, we have

$$\psi_\xi \sim \psi_{\nabla\zeta}(\mathbf{u})\,\psi_{\nabla\zeta}(-\mathbf{v}) \exp\left[-(K\sigma\cot\theta)^2\right] \times \{1 + (K\cot\theta)^2 R + K\cot\theta R_{,\alpha}(u_\alpha - v_\alpha) - R_{,\alpha\beta}u_\alpha v_\beta + \text{second-order terms in } \mu^0\} \tag{37}$$

where $\psi_{\nabla\zeta}(\mathbf{u}) = \exp(-\frac{1}{2}m_{\alpha\beta}u_\alpha u_\beta)$. The second-order terms are carried in the appendix. Now making use of the identities,

$$p_{\nabla\zeta}(\mathbf{s}) = \frac{1}{(2\pi)^2}\int \psi_{\nabla\zeta}(\mathbf{u}) e^{-is\cdot u}\,d\mathbf{u}$$

$$\frac{\partial p_{\nabla\zeta}}{\partial s_\alpha} = \frac{-i}{(2\pi)^2}\int u_\alpha \psi_{\nabla\zeta}(\mathbf{u}) e^{-is\cdot u}\,d\mathbf{u} \tag{38}$$

and so forth, we have for Ξ, (29), on integrating over u and v:

$$\Xi \sim p_{\nabla\zeta}{}^2(\mathbf{s}) \exp\left[-(K\sigma\cot\theta)^2\right] \cdot \left\{1 + (K\cot\theta)^2 R + 2iK\cot\theta\frac{p_{,\alpha}}{p}R_{,\alpha} - \frac{p_{,\alpha}p_{,\beta}}{p^2}R_{,\alpha\beta} + \text{second-order terms in } \mu^0\right\} \tag{39}$$

where for short in the series part of (39) we have let $p \equiv p_{\nabla\zeta}(\mathbf{s})$ and $p_{,\alpha} \equiv \partial p/\partial s_\alpha$, etc.

The moment $M_1(\mathbf{K})$ as given by (28) is the FT of Ξ as seen through the lag window $A(\mathbf{w})$. If $A(\mathbf{w})$ is broad compared to the correlation scale of the waves (as will always be the case in satellite measurements), then the effect of the finite window on the modulation spectrum can be ignored and we can write M_1 as

$$M_1(\mathbf{K}) = (\pi/2r_0{}^2\cos^4\theta)^2 p_{\nabla\zeta}{}^2(\mathbf{s}) \cdot \exp\left[-(K\sigma\cot\theta)^2\right] \times [\mathrm{FT}\{A(\mathbf{w})\} + A(\mathbf{0}) \cdot \mathrm{FT}\{\text{linear + higher-order terms in (39)}\}] \tag{40}$$

where the two-dimensional Fourier transform,

$$\mathrm{FT}\{\cdots\} \overset{\text{def.}}{=} \frac{1}{(2\pi)^2}\int \{\cdots\} e^{-i\mathbf{K}\cdot\mathbf{w}}\,d\mathbf{w} \tag{41}$$

Let the reference axes x_1 and x_2 be fixed in the antenna beam; that is let x_1 be the surface range coordinate, parallel to $\hat{\boldsymbol{\rho}}$ and K, and let x_2 be the orthogonal azimuthal coordinate. Assume a Gaussian gain pattern,

$$G(\mathbf{x}) = \exp\left[-\frac{1}{2}(x_1/L_\rho)^2 - \frac{1}{2}(x_2/L_\phi)^2\right] \tag{42}$$

Then from (22)

$$\mathrm{FT}\{A(\mathbf{w})\} = (2\pi)^{-2} \cdot \iint A(w_1, w_2)\exp(-iKw_1)\,dw_1\,dw_2$$

$$= (L_\rho L_\phi/2)^2 \exp\left[-\frac{1}{2}(KL_\rho)^2\right] \tag{43}$$

Making use of the second-moment result (31) noting that $A(\mathbf{0}) = A_0/2 = \pi L_\rho L_\phi/2$ we write (40) in the form

$$M_1(\mathbf{K}) = \frac{\sqrt{2\pi}}{L_\rho}\,[(|S(k)|^2)]^2 \cdot \left\{\frac{L_\rho}{\sqrt{2\pi}}\exp\left[-\frac{1}{2}(KL_\rho)^2\right] + P_{\text{mod}}(\mathbf{K})\right\} \tag{44}$$

where the modulation spectrum

$$P_{\text{mod}}(\mathbf{K}) = (\sqrt{2\pi}/L_\phi)\exp\left[-(K\sigma\cot\theta)^2\right] \cdot \text{FT}\{\text{linear + higher-order terms in (40)}\} \tag{45}$$

The directional height spectrum is defined by

$$F(\mathbf{K}) = \text{FT}\{R(\mathbf{w})\} \tag{46}$$

Then, since $\text{FT}\{R_{,\alpha}\} = iK_\alpha F(\mathbf{K})$ and $\text{FT}\{R_{,\alpha\beta}\} = -K_\alpha K_\beta F(\mathbf{K})$ the expansion for P_{mod} becomes

$$P_{\text{mod}}(\mathbf{K}) = \frac{\sqrt{2\pi}}{L_\phi}\,e^{-(K\sigma\cot\theta)^2} \cdot \left\{\left[\cot^2\theta - 2\cot\theta\,\frac{p_{,\alpha}}{p}\cdot\frac{K_\alpha}{K} + \frac{p_{,\alpha}p_{,\beta}}{p^2}\cdot\frac{K_\alpha K_\beta}{K^2}\right] \cdot K^2F(\mathbf{K}) + \cdots\right\} \tag{47}$$

or

$$P_{\text{mod}}(\mathbf{K}) = \frac{\sqrt{2\pi}}{L_\phi}\,e^{-(K\sigma\cot\theta)^2} \cdot \left\{\left(\cot\theta - \frac{\partial \ln p}{\partial s}\right)^2 K^2F(\mathbf{K}) + \cdots\right\} \tag{48}$$

where $\partial \ln p/\partial s \equiv (K_\alpha/K)\cdot(p_{,\alpha}/p) \equiv \hat{\boldsymbol{\rho}}\cdot\nabla_s p$. Note that if the exponential factor is neglected (which neglect is consistent with the neglect of the second-order terms) then the linear term of the solution agrees with the simple tilt model of Figure 2. The L_ϕ^{-1} dependence of the solution is a consequence of the large footprint assumption, $KL_\phi \gg 1$, and can be interpreted simply as follows: in a real short-crested sea, the waves are running out-of-step so that the wave modulation signal power adds noncoherently as $L_\phi^{1/2}$ across the footprint. The total backscattered power on the other hand adds directly as L_ϕ. Hence, the relative range modulation power goes as $L_\phi^{-1/2}$ and its spectrum as L_ϕ^{-1}.

To gain some feel for the effect of the second-order terms, sample calculations have been carried out by using (A5) of the appendix assuming a simplified two-dimensional scattering geometry. The results shown in Figure 5 indicate that the second-order terms are generally small. The modulation spectrum bears good fidelity to the surface slope spectrum in the incidence angle range 8°–15° for windspeeds ≥ 5 m s^{-1} and significant wave slopes $\delta_0 \lesssim 0.1$.

MOMENT SOLUTION (FRESNEL ZONE)

We now calculate the moment (10) with $S(k, t)$ given by the physical optics integral in the Fresnel approximation to the phase where we neglect the term in height, $k\zeta^2/r_0$. Proceeding exactly as in the far-zone solution, we form the moment as the four-fold integral over the dummy space variables $\mathbf{x}^1 \cdots \mathbf{x}^4$ and interchange expectation and integration operations. Again we recognize that for large k, significant contributions to the moment are made only in the vicinity of the 'stationary' points defined by (18). The moment M is thus decomposable as $M \simeq M_1 + M_2$ where M_1 and M_2 represent the contributions from $\mathscr{S}_1$ and $\mathscr{S}_2$. Again, we consider the integration over the volume surrounding the $\mathscr{S}_1$ points. Transforming to the lag variables $\mathbf{u}$, $\mathbf{v}$, and $\mathbf{w}$ as per (19) and taking the limit, we get for the contribution from $\mathscr{S}_1$

$$\lim_{k\to\infty} M_1 \equiv M_1(\mathbf{K}; \Delta t) = (2r_0\cos^2\theta)^{-4} \cdot \int\int G^2(\mathbf{x} + \mathbf{w})\,G^2(\mathbf{x} - \mathbf{V}\Delta t) \cdot \Xi(K; \mathbf{w})\exp\left[-i\mathbf{K}\cdot(\mathbf{w} + \mathbf{V}\Delta t)\right]\exp\{i(\kappa/r_0) \cdot [\cos^2\theta((x_1 + w_1)^2 - (x_1 - V_1\Delta t)^2) + (x_2 + w_2)^2 - (x_2 - V_2\Delta t)^2]\}\,d\mathbf{x}\,d\mathbf{w} \tag{49}$$

where we have taken the coordinates x_1 and x_2 of $\mathbf{x}$ to be radar-fixed coordinates (x_1 in the plane of incidence). Let G be the separable Gaussian pattern given by (42). Then integrating over $\mathbf{x}$ we get

$$M_1(\mathbf{K}; \Delta t) = (2r_0\cos^2\theta)^{-4}\int B(K; \mathbf{w} + \mathbf{V}\Delta t) \cdot \Xi(K; \mathbf{w})\exp\left[-i\mathbf{K}\cdot(\mathbf{w} + \mathbf{V}\Delta t)\right]d\mathbf{w} \tag{50}$$

where

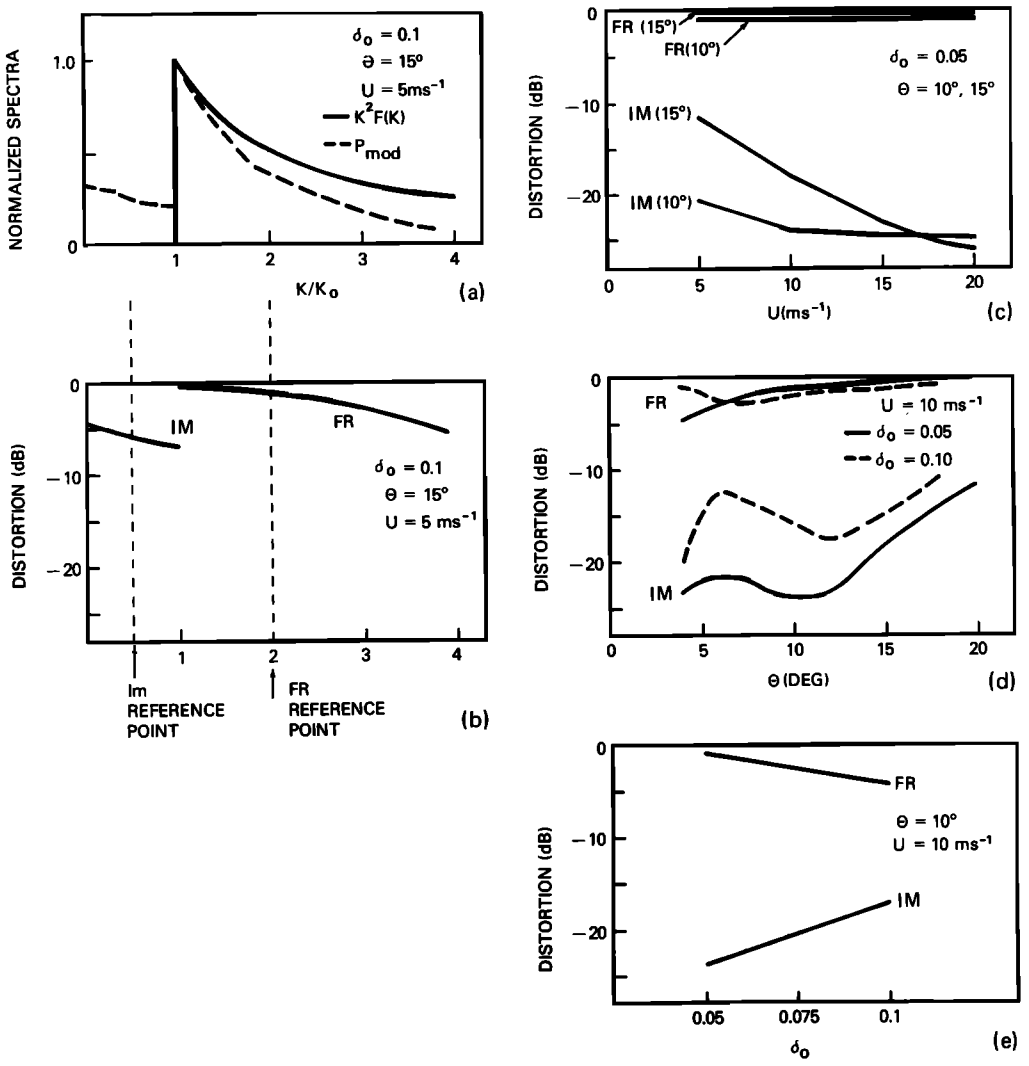

Fig. 5. Sample calculations of the spectrum $P_{mod}(K)$ of backscattered impulses from a Gaussian sea surface in two dimensions in the second order of scattering. (*a*, *b*) The surface slope spectrum $K^2F(K)$ is the Phillips spectral form, BK^{-1}, with an abrupt cutoff at $K = K_0$. The slope spectrum and P_{mod} are both normalized by their values at K_0. The calculations are performed for a range of wave steepness $\delta_0 = K_0\sigma = \sqrt{B/2}$, incidence angle θ and wind speed U (which determines the total mean square slope according to (32)). In all calculations, the location of the peak at K_0 is preserved; low frequency whitening—or intermodulation (IM)—is exhibited, and the frequency response (FR) at wave numbers $K > K_0$ is in the form of a droop. (*c*, *d*, *e*) The variation of the IM at $K = 0.5\ K_0$ and the FR at $K = 2\ K_0$ over the range of parameter values indicated.

$$B(K; \mathbf{w}) = (A_0/2) \exp\left(-\frac{1}{2} b_\alpha^2 w_\alpha^2\right) \tag{51}$$

The illuminated area $A_0 = \pi L_\rho L_\phi$ and the b_α

$$\begin{aligned} b_1^2 \equiv b_\rho^2 &= L_\rho^{-2} + (KL_\rho/2r_0 \sin\theta)^2 \cos^4\theta \\ b_2^2 \equiv b_\phi^2 &= L_\phi^{-2} + (KL_\phi/2r_0 \sin\theta)^2 \end{aligned} \tag{52}$$

Since $M = M_1 + M_2$, then N as given by (11) is similarly composed, i.e., $N = N_1 + N_2$ where N_1 and N_2 are the respective FTs of M_1 and M_2 with respect to Δt. From (11) we have

$$N_1(\mathbf{K}; \Omega) = (2r_0 \cos^2\theta)^{-4} \int d\mathbf{w} \Xi(K; \mathbf{w}) \exp(-i\mathbf{K} \cdot \mathbf{w})$$
$$\times \{(2\pi)^{-1} \int d\Delta t B(K; \mathbf{w} + \mathbf{V}\Delta t)$$

$$\cdot \exp\,[i(\Omega - \mathbf{K}\cdot\mathbf{V})\Delta t]\} \tag{53}$$

Let $\mathscr{W} = (b_1 w_1,\ b_2 w_2)$, $\mathscr{V} = (b_1 V_1,\ b_2 V_2)$ and $\Omega_* = \Omega - \mathbf{K}\cdot\mathbf{V}$. Then integrating over Δt we get

$$N_1(\mathbf{K};\Omega) = \frac{(A_0/2)}{(2r_0\cos^2\theta)^4}\int d\mathbf{w}\Xi(K;\mathbf{w}) \cdot \exp(-i\mathbf{K}\cdot\mathbf{w}) \times \left\{\frac{\exp\left[-\frac{1}{2}(\Omega_*/\mathscr{V})^2\right]}{\sqrt{2\pi}\mathscr{V}} \cdot \exp\left[-\frac{1}{2}\mathscr{W}^2\sin^2(\mathscr{V},\mathscr{W})\right] \cdot \exp\,[i\mathscr{W}\cos(\mathscr{V},\mathscr{W})\Omega_*/\mathscr{V}]\right\} \tag{54}$$

From (11) and the inverse FT relationship it follows that

$$M_1(\mathbf{K};0) = \int N_1(\mathbf{K};\Omega)d\Omega = (2r_0\cos^2\theta)^{-4} \cdot \int B(K;\mathbf{w})\Xi(K;\mathbf{w})\exp(-i\mathbf{K}\cdot\mathbf{w})d\mathbf{w} \tag{55}$$

which is the same as the Fraunhofer solution (28), except that the Fresnel lag window $B(K;\mathbf{w})$ replaces the Fraunhofer lag window $A(\mathbf{w})$. Since B is not significantly sharper than A and the window can still be considered to be broad compared to the scale of variation in Ξ (i.e., broad compared to the dominant wavelength $2\pi/K_0$), then $M_1(\mathbf{K};0)$ can be regarded as identical to the Fraunhofer moment $M_1(\mathbf{K})$. (Note that $B(0;\mathbf{w}) = A(\mathbf{w})$ and $B(K;\mathbf{0}) = A(\mathbf{0}) = A_0/2$.) If the detailed behavior of $N_1(\mathbf{K};\Omega)$ near the origin $\mathbf{K} = 0$ is ignored, then it is apparent that N_1 is well approximated by

$$N_1(\mathbf{K};\Omega) \simeq M_1(\mathbf{K})\cdot\frac{\exp(-\Omega_*^2/2\beta_{res}^2)}{\sqrt{2\pi}\beta_{res}} \tag{56}$$

where M_1 is given by (44), and

$$\beta_{res} \overset{\text{def}}{=} |\mathscr{V}| = (b_\alpha V_\alpha)^{1/2} = (b_\rho^2\cos^2\Phi + b_\phi^2\sin^2\Phi)^{1/2}\cdot V \tag{57}$$

where Φ is the radar azimuth relative to the velocity vector $\mathbf{V}$. In A-H, only the line-broadening due to wave-front curvature was considered (i.e., it was assumed that $\beta_{res} \simeq \kappa LV/r_0$). However, to be accurate, the broadening due to the finite footprint must be accounted for also. Thus, compare V/L and $\kappa LV/r_0$ for typical aircraft and satellite geometries and ocean wavelengths: both terms are comparable.

The moment $M(k,\Delta k,\kappa;\Delta t)$ is not symmetric with respect to a κ and Δk interchange, and so the M_2 component (deriving from the $\mathscr{S}_2$ stationary points) cannot simply be equated to M_1, as was possible in the time-independent case. Rather than labor through a solution for M_2 in these pages, we merely outline the key steps in the solution and indicate the appropriate assumptions and approximations: lag variables appropriate to the $\mathscr{S}_2$ integration are defined, and the $k\to\infty$ limit is taken in the formation of Ξ; the Fresnel phase terms in κ and Δk are neglected; assuming a large footprint area, we neglect the variation of Ξ near the origin and let $\Xi \sim \Xi(0;\infty) = p_{\nabla\zeta}{}^2(\mathbf{s})$ in the integration over $\mathbf{w}$. Then, on taking the FT of M_2, we get

$$N_2 \simeq [\langle|S(k)|^2\rangle]^2\exp\left[-\frac{1}{2}(q\Delta KL_\rho)^2\right]\cdot\frac{\exp\left[-\frac{1}{2}(\Omega_*/\beta_d)^2\right]}{\sqrt{2\pi}\beta_d}\cdot\exp(i\varepsilon\Omega_*/\beta_d^2) \tag{58}$$

where

$$q = |\sin\Phi|\cdot[(L_\rho/L_\phi)^2\cos^2\Phi + \sin^2\Phi]^{-1/2}$$
$$\beta_d = (2kV/r_0)\cdot[L_\rho^2\cos^4\theta\cos^2\Phi + L_\phi^2\sin^2\Phi]^{1/2}$$
$$\varepsilon = (2kV/r_0)\cdot\Delta KL_\rho^2\cos^2\theta\cos\Phi \tag{59}$$

and where $\Delta K \equiv 2\Delta k\sin\theta$. As a check on (58) we have

$$\int_{-\infty}^{\infty} N_2 d\Omega = [\langle|S(k)|^2\rangle]^2\exp\left[-\frac{1}{2}(\Delta KL_\rho)^2\right] \tag{60}$$

which is $M_1(\Delta\mathbf{K})$ with the weak modulation contribution neglected.

SNR ANALYSIS

By the SNR is meant the ratio of the average output signal of the systems of Figures 3 and 4 (i.e., the estimate of the modulation spectrum) to the broad fading spectrum that exists in the absence of signal modulation. We do not consider here the additional contribution to the noise background made by thermal noise.

DF technique. The spectrum of the DF signal is simply $N = N_1 + N_2$ with ΔK set equal to zero in N_2 (Since $\nu = \nu'$, then $\Delta\nu = \Delta K = 0$). Since the Doppler spread β_d is large compared with the Doppler shift frequency of the modulation, it follows that in the vicinity of the 'resonance' peak at $\Omega = \mathbf{K} \cdot \mathbf{V}$ we can take $N_2 \sim 1/\sqrt{2\pi}\beta_d$. Let us consider short integration times $T_{\text{int}} \ll 2\pi\beta_{\text{res}}^{-1}$ such that the spectral window $W(\Omega)$ entirely covers the resonance peak. Then the spectral estimate computed at the Doppler frequency $\Omega = \mathbf{K} \cdot \mathbf{V}$ is given by (cf. (13))

$$\tilde{P} \equiv \tilde{P}_1 + \tilde{P}_2 \simeq W(0) \int N_1 d\Omega + N_2 \int W d\Omega$$

$$= (1) \cdot \frac{\sqrt{2\pi}}{L_\rho} P_{\text{mod}}(\mathbf{K}) + \frac{1}{\sqrt{2\pi}\beta_d}\left(\frac{2\pi^2}{T_{\text{int}}}\right) \tag{61}$$

For example, let $T_{\text{int}} = \beta_{\text{res}}^{-1}$. Then the

$$\text{SNR} \equiv \tilde{P}_1/\tilde{P}_2 = 2^{-1/2}\pi^{-3/2}\left(\frac{\beta_d}{\beta_{\text{res}}}\right) \cdot \frac{\sqrt{2\pi}}{L_\rho} P_{\text{mod}}(\mathbf{K}). \tag{62}$$

Our theoretical analysis indicates, and aircraft data, to be published, confirm that the linearized geometrical optics solution for P_{mod} is quite accurate:

$$P_{\text{mod}}(\mathbf{K}) = \frac{\sqrt{2\pi}}{L_\phi}\left(\cot\theta - \frac{\partial \ln p}{\partial s}\right)^2 K^2 F(\mathbf{K}) \tag{63}$$

Let F be given by the Phillips' cutoff spectral form with a $\cos^4\Phi$ spreading factor:

$$F(\mathbf{K}) = 0.005(4/3\pi)\cos^4\Phi K^{-4},$$

$$K \geq K_0 \sim 10/U^2, \text{ and 0 otherwise} \tag{64}$$

Assume upwave/downwave looks, $\Phi = 0$, and assume that the waves and wind are aligned so that the major axis of the Gaussian slope pdf $p = p_{\nabla s}(\mathbf{s})$ coincides both with the radar azimuth and the wind direction. Then $\partial \ln p/\partial s = -\tan\theta/m_{11}$. Assume an axial ratio $m_{11}/m_{22} = 1.5$ according to *Cox and Munk* [1954]; then $m_{11} = 0.6\, m_0^2$ where m_0 is given in terms of windspeed by (32). Assume, for example, the following parameter values:

$$\begin{aligned} r_0 &= 700 \text{ km} \\ V &= 7 \text{ km s}^{-1} \\ \theta &= 10^\circ \\ L_\rho &= L_\phi = 5 \text{ km} \end{aligned} \tag{65}$$

$$\begin{aligned} k &= 2\pi/2 \text{ cm} \\ K &= K_0 = 2\pi/200 \text{ m} \\ U &= 15 \text{ m s}^{-1} \end{aligned}$$

Then the two-sided modulation spectrum,

$$P_{\text{mod}} = (5 \times 10^{-4} \text{ m}^{-1})(5.7 + 6.1)^2(2.1 \text{ m}^2) = 0.15 \text{ m} \tag{66}$$

From (52) we have $b_\rho \sim b_\phi = 6.8 \times 10^{-4}$ m^{-1} and so $\beta_{\text{res}} = 4.7$ rad s^{-1} and $\beta_d = 3.1 \times 10^4$ rad s^{-1}. The value of β_{res} implies $T_{\text{int}} = \beta_{\text{res}}^{-1} = 0.21$ s. Without the filtering the SNR can be considered to be $\text{SNR} = (\sqrt{2}\pi/L_\rho)P_{\text{mod}} = -41$ dB. The A-H filtering gain is then $(2\pi^3)^{-1/2}(\beta_d/\beta_{\text{res}}) = +26$ dB, and the final measurement SNR is accordingly

$$\text{SNR}_{\text{DF}} = -15 \text{ dB} \tag{67}$$

Of course this figure can be improved upon somewhat by designing a spectral analysis with a better match to the resonance peak. However it is clear that given reasonable parameter values the narrowband DF SNR is not likely to exceed 0 dB.

SP technique. Let us write the results (44), (56), and (58) in the frequency domain making use of (1) and (14) and the additional identities $\Delta K \equiv (2\Delta\nu/c)\sin\theta$, $T_r \equiv (2L_\rho/c)\sin\theta$, and $P_{\text{mod}}(\omega, \Phi) \equiv P_{\text{mod}}(\mathbf{K})dK/d\omega$:

$$N_1 = [\langle|S(\nu)|^2\rangle]^2 \cdot \frac{\exp(-\Omega_*^2/2\beta_{\text{res}}^2)}{\sqrt{2\pi}\beta_{\text{res}}} \cdot \frac{\sqrt{2}\pi}{T_r} P_{\text{mod}}(\omega, \Phi) \tag{68}$$

$$N_2 = [\langle|S(\nu)|^2\rangle]^2 \frac{\exp(-\Omega_*^2/2\beta_d^2)}{\sqrt{2\pi}\beta_d} \cdot \exp\left[-\frac{1}{2}(q\Delta\nu T_r)^2\right] \cdot \exp(i\varepsilon\Omega_*/\beta_d) \tag{69}$$

If the pulse bandwidth is large compared to $(qT_r)^{-1}$ then N_2 behaves as a delta function in $\Delta\nu = \nu - \nu'$. Hence, since $\langle|S(\nu)|^2\rangle$ is practically a constant over the pulse bandwidth, (12) becomes

$$P(\omega, \Omega) \equiv P_1 + P_2 = N_1 \cdot \left|\int E_0(\nu)E_0^*(\nu - \omega)d\nu\right|^2 + \left[\int E_0^2(\nu)E_0^2(\nu - \omega)d\nu\right] \cdot \int N_2 d\Delta\nu \tag{70}$$

Making use of the definitions (59) and the identity $\Delta K L_\rho \equiv \Delta\nu T_r$ we have for the N_2 integration,

$$\int N_2 d\Delta\nu = (\sqrt{2\pi}/T_r)[\langle|S(\nu)|^2\rangle]^2 \cdot \frac{\exp\left[-\frac{1}{2}(\Omega_*/q\beta_d)^2\right]}{\sqrt{2\pi}\, q\beta_d} \tag{71}$$

where from (59) it follows that

$$q\beta_d = (2kV/r_0)L_\phi\,|\sin\Phi| \tag{72}$$

which is the Doppler spread due to azimuthal aspect variation alone.

Pulse waveforms are often Gaussian in shape. Let $E_0(\nu)$ at baseband be given by

$$E_0(\nu) = \frac{\exp(-\nu^2/2\beta_p^2)}{\sqrt{2\pi}\beta_p} \tag{73}$$

Then computing the integrals in (70) we have

$$P(\omega, \Omega) = P_1 + P_2 = \frac{\sqrt{2\pi}}{T_r}[\langle|S(\nu)|^2\rangle]^2 \cdot \frac{\exp(-\omega^2/2\beta_p^2)}{4\pi\beta_p^2} \times \left[\frac{\exp(-\Omega_*^2/2\beta_{res}^2)}{\sqrt{2}\pi\beta_{res}} \cdot P_{mod}(\omega, \Phi) + \frac{\exp(-\Omega_*^2/2q^2\beta_d^2)}{2\pi q\beta_d\beta_p}\right] \tag{74}$$

The post-detection 'pulse-Doppler' spectrum $P(\omega, \Omega)$ is sketched in Figure 6.

Except for looks directly forward ($\Phi = 0°$) or aft ($\Phi = 180°$), $q\beta_d \gg \beta_{res}$. Hence, in the vicinity of the resonance peak at $\Omega = \mathbf{K} \cdot \mathbf{V}$ we can set $\Omega_* = 0$ in P_2. Again, if we assume short integration times T_{int} such that the resonance peak is entirely covered by the spectral window W, the filtered pulse spectrum becomes,

$$\tilde{P}(\omega) \equiv \tilde{P}_1 + \tilde{P}_2 \simeq W(0)\int P_1 d\Omega + P_2 \int W d\Omega \tag{75}$$

Again assume that $T_{int} = \beta_{res}^{-1}$. Then the SNR $\equiv \tilde{P}_1/\tilde{P}_2$ becomes

$$\mathrm{SNR}_{SP} = 2^{-1/2}\pi^{-3/2}(q\beta_d/\beta_{res})\underbrace{\sqrt{2\pi}\beta_p P_{mod}(\omega, \Phi)}_{\equiv (\sqrt{2\pi}/\Delta\rho)P_{mod}(\mathbf{K})} \tag{76}$$

where $\Delta\rho$ is the bandwidth-equivalent surface range resolution. In the absence of pulse integration or in the limit $T_{int} \to 0$, the pulse spectrum is given by $P(\omega) = \int P(\omega, \Omega)\, d\Omega$. That is, the ensemble average spectrum of individual backscattered pulses is given by collapsing $P(\omega, \Omega)$ upon the fast frequency axis (cf. Figure 6). Evidently from (74) the

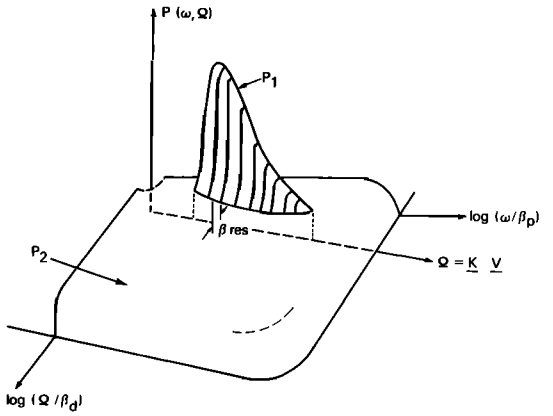

Fig. 6. Post-detection 'pulse-Doppler' spectrum.

SNR in the 'unfiltered' case is SNR $= \int P_1 d\Omega / \int P_2 d\Omega = \sqrt{2\pi}\beta_p P_{mod}$. For example let $\Delta\rho =$ 5 m. Then with P_{mod} given by (65), the unfiltered SNR $= -11$ dB. Because of the pulse-limited illumination, the filtering gain in the SP measurement is a rather strong function of azimuth. In the equal beamwidth case we are considering the gain goes as $q = |\sin\Phi|$. For broadside looks the final measurement SNR $= +26$ dB $- 11$ dB $= +15$ dB, and for any azimuth,

$$\mathrm{SNR}_{SP} = +15\ \mathrm{dB} + 10\log|\sin\Phi| \tag{77}$$

The SNR is 0 dB for look $\pm 2°$ of directly forward or aft. In addition to the SNR one is interested to know the actual modulation signal strength. The rms modulation depth or 'contrast ratio' is given by

$$CR = \left[2\int_{K_0}^{\infty} P_{mod}(\mathbf{K})\, dK\right]^{1/2} = 10\% \tag{78}$$

which follows from (63) and (64) assuming $K_0 = 2\pi/200$ m. The upper limit strictly applies to impulses; however, the CR is not materially altered if the upper limit is replaced by wave numbers corresponding to range resolutions in the 5-m range as is evident from (64).

Before concluding here we remark on the high directional resolution of the measurements we are considering. Directional resolution is determined by the combination of finite footprint and wavefront curvature factors that is embodied in the Fresnel lag window (51). From (51) the lateral wave number uncertainty is $\delta K_2 = b_\phi$. Since b_ϕ is small, the directional uncertainty of a given wave vector $\mathbf{K}$

$= (K_1, K_2)$ is $\delta\Phi \sim \delta K_2/K$. The half-power spectral window width is then equal to $2(2 \ln 2)^{1/2} b_\Phi / K$. For the typical 200 m water wave we have

$$\delta\Phi = 0.92° \tag{79}$$

Such a high resolution suggests the advisability of scanning nearly continuously in azimuth, otherwise very narrowly directed swell systems may go undetected.

CONCLUSION

A few points deserve, or require, comment. First, regarding the geometrical optics approximation: this is bound to be quite accurate in the present context because the diffraction field, in addition to being small, is comparatively diffuse as well [*Brown*, 1978]. Thus it can contribute only negligibly to the modulation via the tilt mechanism. Diffraction acts mainly to reduce the rms surface slope that is effective in the specular scatter component by inhibiting specular reflections from waves smaller than the diffraction limit, which limit according to *Brown* [1978] is about three electromagnetic wavelengths in the horizontal. In this connection it is worth noting that those waves that are most strongly forced, the gravity-capillary waves, lie under the diffraction limit for 2–3 cm radars.

Not mentioned in the text is the fact that the moment solution (28)–(30) does not exist in the strict mathematical sense. $\Xi(K; \mathbf{w})$ is singular at the origin $\mathbf{w} = 0$ because the joint pdf of slopes is singular. From the definition of a joint pdf it follows that for any smooth surface the joint pdf must go as w^{-1} as $w \to 0$. Hence $M_1(\mathbf{K})$ is logarithmically divergent. Physically, the singularity is due to the point source approximation which is implicit in the physical optics integral formulation (14). In the case of a point source, the cross section of a specular point is proportional to the reciprocal of Gaussian surface curvature. As shown by *Longuet-Higgins* [1959] the reciprocal curvature has unbounded variance, and so the variance of specularly reflected power is also unbounded. Of course, the singularity at the origin can be removed by accounting for the finiteness of the source; however, in the present context the problem of representation at the origin is regarded as basically trivial on account of the large areas and numbers of specular points involved.

Assuming Gaussian surface statistics, we have carried out an expansion of the moment solution explicitly to second order, and we have shown that the harmonic distortion introduced into a measurement of the surface slope spectrum by the second-order terms is generally small, provided sufficient small-scale roughness (windspeed $\gtrsim$ 5 m s^{-1}). Minimum harmonic distortion obtains near 10° incidence, or in the vicinity of least sensitivity of $\sigma°(\theta)$ to changes in the rms slope, m_0. A rough accounting of non-Gaussian 'skewness' statistics indicates that these statistics can produce distortions in the measured height or slope spectrum of comparable magnitude to those existing in the second order of scattering from a normally distributed sea. Thus, if the problem of measurement nonlinearities is to be addressed seriously, non-Gaussian wave statistics must be considered. Fortunately, the nonlinearities are small, and it is averred that rather accurate measurements of the directional height spectrum can be made simply by using the linearized 'tilt model' solution, (63). In fact, aircraft data, to be published, show this to be the case.

If thermal noise is not a factor affecting the measurement, then it is evident from our analysis that the SP technique is much superior to the narrowband DF technique. The truth of this statement becomes even more transparent when one considers that each DF measurement is subject to a 100% sampling variability because there is no frequency averaging. Thus even with a dozen or more channels operating simultaneously one is stuck for integration time. In view of the wavefield homogeneity problem, one must accomplish an azimuth scan within the time it takes to travel ~100 km. This leaves ~15 s/360° = 0.04 s of integration time available for a 1° azimuth look. (Here we are assuming that it is the spectral window width $\delta\Phi$ that determines the allowable movement in azimuth during an integration time interval. This may not be the correct number, but it is probably not far off.) This is to be compared with the 0.2 s allowed in arriving at (67).

In the SP measurement one is also short on integration time, but not nearly so badly. For example, let us consider an actual piece of space-qualified microwave hardware, the Seasat-1 altimeter transmitter [*Townsend*, 1980]. This Ku-band transmitter puts out a 2.5 kw, 300 MHz chirped pulse at a 1 KHz rate. The bandwidth parameter for this waveform $\beta_p \sim 5 \times 10^8$ rad s^{-1} and the range resolution parameter $\Delta\rho = c/(2\beta_p \sin\theta) \sim$ 1.7 m at 10° incidence. Hence the unfiltered SNR

~ -7 dB for the 200 m water wave example. Because the PRF in this case is lower than the Doppler bandwidth, we cannot use the results of the continuous analysis. Because the signal is undersampled, the fading spectrum $P_2(\omega, \Omega)$ will be folded-over on itself at intervals of the Nyquist frequency Ω_N = PRF ÷ 2. The measured fading spectrum level will accordingly be increased in proportion to the Doppler bandwidth divided by the PRF. Now since outside of two sectors of some given width centered at 0° and 180° the PRF is lower than the Doppler bandwidth, it follows that the backscattered pulses are independent vis-a-vis the fading statistics, and so the result of integrating N pulses is simply to reduce the fading variance by a factor of N^{-1}. Given the Seasat-1 altimeter PRF of 1 KHz, and allowing 0.04 s integration time, then $N = 40$ pulses are put on target, and so the integration gain will be +16 dB. Hence the final measurement SNR $\sim$ +16 dB − 7 dB = +9 dB. This SNR will be constant outside of the foreward and aft sectors where the Doppler bandwidth drops below the PRF.

It was said in the introduction that the solution to the low SNR problem in the DF technique was to use signals with bandwidths commensurate with the modulation spectrum bandwidth. Yet we have not found the space here to describe or analyze such possible systems. Why? Apart from space limitation, the reason is that SP systems such as the Seasat-1 altimeter can deliver a better-than-unity signal-to-thermal-noise ratio, and basically this is all that is required in order that thermal noise not seriously degrade the measurement SNR. Thus, while ultimately such factors as transmitter tube life may warrant a detailed trade-off analysis of wideband DF and SP systems, at present the motivation for such an analysis is lacking.

APPENDIX: SECOND-ORDER TERMS IN THE EXPANSION OF $M_1(\mathbf{K})$

The second-order terms in the expansion of ψ_ξ, (37), are

$$\frac{1}{2}\left[\frac{1}{2}\mu_{ij}^{0} t_i t_j\right]^2 \equiv \frac{1}{8}\mu_{ij}^{0}\mu_{kl}^{0} t_i t_j t_k t_l$$

$$= \frac{1}{2}\left[(K\cot\theta)^4 R^2 + R_{,\alpha\beta} R_{,\gamma\delta} u_\alpha u_\delta v_\beta v_\gamma \right.$$

$$+ (K\cot\theta)^2 R_{,\alpha} R_{,\beta}(u_\alpha u_\beta - 2u_\alpha v_\beta + v_\alpha v_\beta)$$

$$- 2(K\cot\theta)^2 R R_{,\alpha\beta} u_\alpha v_\beta + 2(K\cot\theta)^3 R R_{,\alpha}(u_\alpha - v_\alpha)$$

$$\left. - 2(K\cot\theta) R_{,\alpha\beta} R_{,\gamma} u_\alpha v_\beta (u_\gamma - v_\gamma)\right] \tag{A1}$$

Fourier transforming with respect to $\mathbf{u}$ and $\mathbf{v}$ according to (29) and making use of the identities (38), we get for the second-order terms in the expansion of Ξ, (39):

$$\frac{1}{2}(K\cot\theta)^4 R^2 + \frac{1}{2}\frac{p_{,\alpha\delta} p_{,\beta\gamma}}{p^2} R_{,\alpha\beta} R_{\gamma\delta}$$

$$- (K\cot\theta)^2\left(\frac{p_{,\alpha\beta}}{p} + \frac{p_{,\alpha} p_{,\beta}}{p^2}\right) R_{,\alpha} R_{,\beta}$$

$$- (K\cot\theta)^2 \frac{p_{,\alpha} p_{,\beta}}{p^2} R R_{,\alpha\beta}$$

$$+ 2i(K\cot\theta)^3 \frac{p_{,\alpha}}{p} R R_{,\alpha} - iK\cot\theta$$

$$\cdot \left(\frac{p_{,\alpha\gamma} p_{,\beta} + p_{,\beta\gamma} p_{,\alpha}}{p^2}\right) R_{,\alpha\beta} R_{,\gamma} \tag{A2}$$

From the definition of the height spectrum as the Fourier transform of the covariance function, viz.,

$$F(\mathbf{K}) \equiv \mathrm{FT}\{R\} \equiv \frac{1}{(2\pi)^2}\int R(\mathbf{w}) e^{-i\mathbf{K}\cdot\mathbf{w}} d\mathbf{w} \tag{A3}$$

it follows that the FT of the second-order terms in Ξ is given by various convolutions involving the height spectrum; e.g.,

$$\mathrm{FT}\{R R_{,\alpha}\} = \mathrm{FT}\{R\} * \mathrm{FT}\{R_{,\alpha}\}$$

$$= F(\mathbf{K}) * [iK_\alpha F(\mathbf{K})]$$

$$\equiv \int_{-\infty}^{\infty} F(\mathbf{K}')[i(K'_\alpha - K_\alpha) F(\mathbf{K}' - \mathbf{K})]\, d\mathbf{K}' \tag{A4}$$

If an overbar is used to distinguish a variable wavenumber entering into a convolution, then the second-order terms in the expansion of P_{mod}, (49), are written as

$$+\frac{1}{2}(K\cot\theta)^4 F * F + \frac{1}{2}\frac{p_{,\alpha\delta} p_{,\beta\gamma}}{p^2}\overline{K_\alpha K_\beta F} * \overline{K_\gamma K_\delta F}$$

$$+ (K\cot\theta)^2\left(\frac{p_{,\alpha\beta}}{p} + \frac{p_{,\alpha} p_{,\beta}}{p^2}\right)\overline{K_\alpha F} * \overline{K_\beta F}$$

$$+ (K\cot\theta)^2 \frac{p_{,\alpha} p_{,\beta}}{p^2} F * \overline{K_\alpha K_\beta F} - 2(K\cot\theta)^3$$

$$\cdot \frac{p_{,\alpha}}{p} F * \overline{K_\alpha F} - K\cot\theta\left(\frac{p_{,\alpha\gamma} p_{,\beta} + p_{,\beta\gamma} p_{,\alpha}}{p^2}\right)$$

$$\cdot \overline{K_\alpha K_\beta F} * \overline{K_\gamma F} \tag{A5}$$

REFERENCES

Alpers, W., and K. Hasselmann (1978), The two-frequency microwave technique for measuring ocean wave spectra from an airplane or satellite, *Boundary Layer Meteorol., 13,* 215–230.

Barrick, D. E. (1968), Relationship between slope probability density function and the physical optics integral in rough surface scattering, *Proc. IEEE, 56,* 1728–1729.

Beckmann, P., and A. Spizzichino (1963), *The Scattering of Electromagnetic Waves from Rough Surfaces,* 503 pp., Pergamon, New York.

Brown, G. S. (1978), Backscattering from a Gaussian-distributed perfectly conducting rough surface, *IEEE Trans. Antenna Propagat., AP-26,* 472–482.

Cox, C., and W. Munk (1954), Measurement of the roughness of the sea surface from photographs of the sun's glitter, *J. Opt. Soc. Am., 44,* 838–850.

Hasselmann, K., W. Munk, and G. MacDonald (1963), Bispectra of ocean waves, in *Time Series Analysis,* edited by M. Rosenblatt, pp. 125–139, John Wiley, New York.

Jackson, F. C. (1974), Directional spectra of ocean waves from microwave backscatter, in *Proceedings USRI Specialists Meeting Microwave Scattering and Emission from the Earth,* edited by E. Shanda, pp. 257–272, Institute of Applied Physics, University of Berne, Berne, Switzerland.

Jackson, F. C. (1979), The reflection of impulses from a nonlinear random sea, *J. Geophys. Res., 84,* 4939–4943.

Jones, W. L., L. C. Schroeder, and J. L. Mitchell (1977), Aircraft measurements of the microwave scattering signature of the ocean, *IEEE J. Oceanic Eng., OE-2,* 52–61.

Longuet-Higgins, M. S. (1959), The distribution of the sizes of images reflected in a random surface, *Proc. Camb. Phil. Soc., 55,* 91–100.

Longuet-Higgins, M. S. (1963), The effect of nonlinearities on statistical distributions in the theory of sea waves. *J. Fluid Mech., 17,* 459–480.

Papoulis, A. (1965), *Probability, Random Variables, and Stochastic Processes,* pp. 312–318, McGraw-Hill, New York.

Parzen, E., and N. Shiren (1956), Analysis of a general system for the detection of amplitude modulated noise, *J. Math. Phys., 35,* 278–288.

Ruck, G., D. E. Barrick, and T. T. Kaliszewski (1972), Bistatic sea state monitoring, *Tech. Rep.,* Battelle Columbus Lab., Columbus, Ohio.

Townsend, W. F. (1980), An initial assessment of the performance achieved by the Seasat-1 radar altimeter, *IEEE J. Oceanic Eng., OE-5,* 80–92.

Valenzuela, G. R. (1978), Theories for the interaction of electromagnetic and oceanic waves—A review, *Boundary Layer Meteorol., 13,* 61–85.

Wright, J. W., W. J. Plant, W. C. Keller, and W. L. Jones (1980), Ocean wave-radar modulation transfer functions from the West Coast Experiment, *J. Geophys. Res., 85,* 4957–4966.